Mimicking Protein−Protein Electron Transfer: Voltammetry of *Pseudomonas aeruginosa* Azurin and the *Thermus thermophilus* Cu$_A$ Domain at ω-Derivatized Self-Assembled-Monolayer Gold Electrodes

Kyoko Fujita,[†,‡] Nobufumi Nakamura,[‡] Hiroyuki Ohno,[‡] Brian S. Leigh,*,[†]
Katsumi Niki,[†] Harry B. Gray,[†] and John H. Richards*,[†]

Contribution from the Division of Chemistry and Chemical Engineering, California Institute of Technology, Pasadena, California 91125, and Department of Biotechnology, Tokyo University of Agriculture and Technology, Koganei, Tokyo 184-8588, Japan

Received April 13, 2004; E-mail: jhr@its.caltech.edu; bleigh@caltech.edu

Abstract: Well-defined voltammetric responses of redox proteins with acidic-to-neutral pI values have been obtained on pure alkanethiol as well as on mixed self-assembled-monolayer (SAM) ω-derivatized alkanethiol/gold bead electrodes. Both azurin (*P. aeruginosa*) (pI = 5.6) and subunit II (Cu$_A$ domain) of *ba$_3$*-type cytochrome *c* oxidase (*T. thermophilus*) (pI = 6.0) exhibit optimal voltammetric responses on 1:1 mixtures of [H$_3$C(CH$_2$)$_n$SH + HO(CH$_2$)$_n$SH] SAMs. The electron transfer (ET) rate vs distance behavior of azurin and Cu$_A$ is independent of the ω-derivatized alkanethiol SAM headgroups. Strikingly, only wild-type azurin and mutants containing Trp48 give voltammetric responses: based on modeling, we suggest that electronic coupling with the SAM headgroup (H$_3$C− and/or HO−) occurs at the Asn47 side chain carbonyl oxygen and that an Asn47-Cys112 hydrogen bond promotes intramolecular ET to the copper. Inspection of models also indicates that the Cu$_A$ domain of *ba$_3$*-type cytochrome *c* oxidase is coupled to the SAM headgroup (H$_3$C− and/or HO−) near the main chain carbonyl oxygen of Cys153 and that Phe88 (analogous to Trp143 in subunit II of cytochrome *c* oxidase from *R. sphaeroides*) is not involved in the dominant tunneling pathway. Our work suggests that hydrogen bonds from hydroxyl or other proton-donor groups to carbonyl oxygens potentially can facilitate intermolecular ET between physiological redox partners.

Introduction

Self-assembled monolayers (SAM) of organosulfur compounds on metal surfaces have wide applications due to their versatility in modifying surfaces in a controllable manner. Densely packed ω-derivatized alkanethiol SAMs are thermodynamically stable and mechanically robust. The physicochemical properties of SAM surfaces (acid−base and chemical properties, wettability, biocompatibility, and others) are controlled by varying the ω-functional groups. Great diversity in surface properties is attainable using mixed SAMs composed of two or more thiols with different ω-functional groups and chain lengths. In a series of important papers, Whitesides and others reported the composition, structure, and wettability of SAMs with multiple functional groups.[1−5] Though electrochemically inactive themselves, these SAMs act as electron tunneling wires as well as provide specific binding sites for the redox proteins.[6−11]

It is well established that cytochrome *c* (cyt *c*) is immobilized electrostatically on HOOC-SAMs and that desorption of the protein from the surface into electrolyte solutions is negligible at low ionic strengths (<50 mM phosphate buffer solution in the pH range 6−9).[8,9] Van Duyne and co-workers investigated the conformation of cyt *c* immobilized on HOOC-SAM/(silver film over nanosphere) electrodes using surface enhanced resonance Raman spectroscopy.[12] With these electrodes, they found that electrostatically bound cyt *c* retains its native structure and function and that binding orients the heme edge toward the electrode surface. In related work, Gaigalas reported a reversible voltammetric response from an acidic protein, *Pseudomonas aeruginosa* azurin, on an alkanethiol self-assembled mono-

---

† California Institute of Technology.
‡ Tokyo Univeristy of Agriculture and Technology.
(1) Bain, C. D.; Evall, J.; Whitesides, G. M. *J. Am. Chem. Soc*. **1989**, *111*, 7155−7164.
(2) Bain, C. D.; Whitesides, G. M. *J. Am. Chem. Soc*. **1989**, *111*, 7164−7175.
(3) Folkers, J. P.; Laibinis, P. E.; Whitesides, G. M. *Langmuir* **1992**, *8*, 1330−1341.
(4) Laibinis, P. E.; Nuzzo, R. G.; Whitesides, G. M. *J. Phys. Chem*. **1992**, *96*, 5097−5105.
(5) Atre, S. V.; Leidberg, B.; Allara, D. L. *Langmuir* **1995**, *11*, 3882−3893.

(6) Tralov, M. J.; Bowden E. F. *J. Am. Chem. Soc*. **1991**, *113*, 1847−1849.
(7) Song, S.; Clark, R. A.; Bowden, E. F.; Tarlov, M. J. *J. Phys. Chem*. **1993**, *97*, 6564−6572.
(8) Feng, Z. Q.; Imabayashi, S.; Kakiuchi, T.; Niki, K. *J. Chem. Soc., Faraday Trans*. **1997**, *93*, 1367−1370.
(9) Avila, A.; Gregory, B. W.; Niki, K.; Cotton, T. M. *J. Phys. Chem. B* **2000**, *104*, 2759−2766.
(10) (a) Niki, K. *Electrochemistry* **2002**, *70*, 82−90. (b) Niki, K.; Sprinkle J. R.; Margoliash, E. *Bioelectrochemistry* **2002**, *55*, 37−40. (c) Niki, K.; Pressler, K. R.; Sprinkle J. R.; Li, H.; Margoliash, E. *Elektrokhimiya* **2002**, *38*, 74−78.
(11) Niki, K.; Hardy, W. R.; Hill, M. G.; Li, H.; Sprinkle, J. R.; Margoliash, E.; Fujita, K.; Tanimura, R.; Nakamura, N.; Ohno, H.; Richards, J. H.; Gray, H. B. *J. Phys. Chem. B*. **2003**, *107*, 9947−9949.
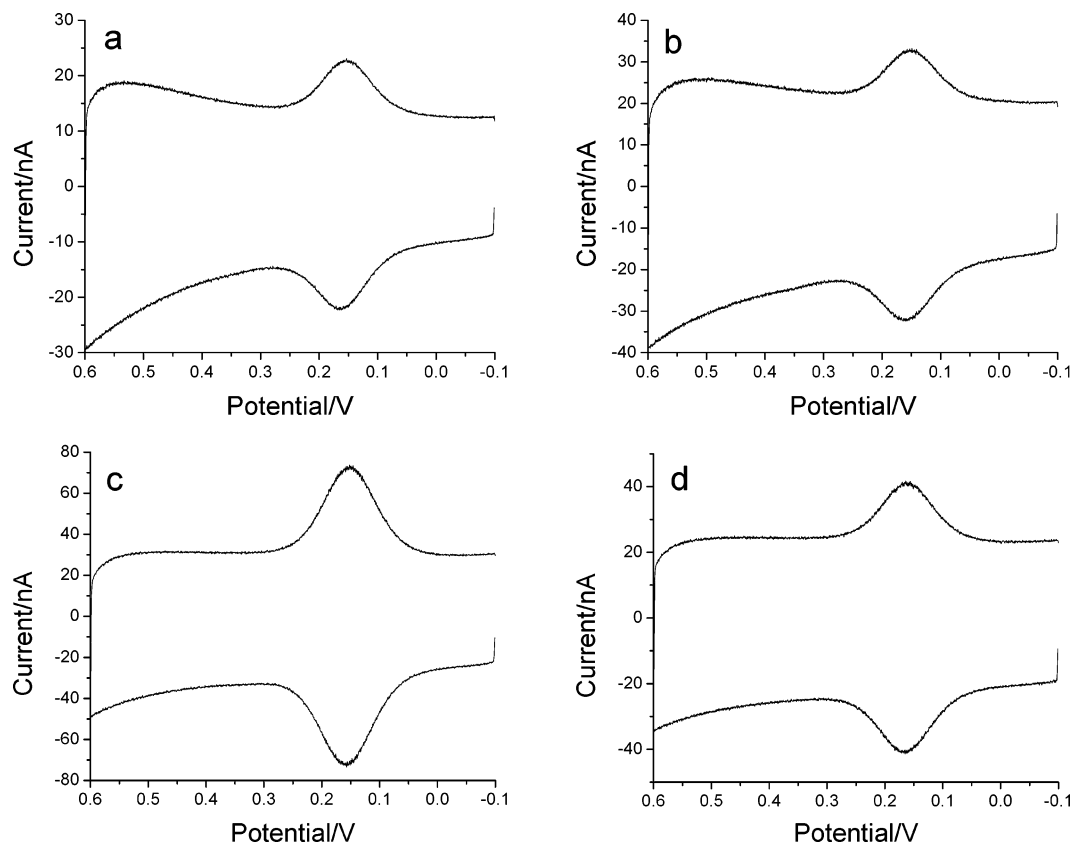(12) Dick, L. A.; Haes, A. M.; Van Duyne, R. P. *J. Phys. Chem. B* **2000**, *104*, 11752−11762.

Figure 1. Cyclic voltammograms of azurin on [$CH_3(CH_2)_8SH$ + $HO(CH_2)_8SH$] SAMs in 10 mM NH_4Ac solution at pH 4.6. Scan rate 50 mV/s; potential vs Ag/AgCl. [$CH_3(CH_2)_8SH$ + $HO(CH_2)_8SH$] mixing ratio (a) 100:0; (b) 3:1; (c) 1:1; (d) 1:3.

layer (H$_3$C-SAM).[13] Notably, Ulstrup and co-workers recently published a comprehensive report on the electrochemistry of azurin on H$_3$C-SAM/gold electrodes.[14,15]

We have investigated the voltammetric responses *P. aeruginosa* azurin and subunit II (the Cu$_A$-domain) from *Thermus thermophilus* cytochrome *c* oxidase (CcO) on mixed ω-derivatized alkanethiol SAM electrodes. Azurin (14.6 kDa, pI = 5.6[16]) is a blue copper protein with two hydrophobic segments on its surface that have been suggested as potential candidates for intermolecular coupling sites.[17] One segment, containing His117, which is a copper ligand and exposed to the solvent, has been implicated in the electron self-exchange reaction[16,18–21] as well as in intermolecular ET with a nitrite reductase.[17] The other hydrophobic patch, which surrounds His35, may serve to couple the protein to cyt *c*$_{551}$.[17] Based on the electron self-exchange rates of Met44Lys and Met64Glu azurins, as well as the voltammetric response of the latter mutant, it has been suggested that His117 is likely to be a prominent azurin electron entry/exit site on the protein surface.[22]

We have shown in our work on cyt *c* that it is possible to pinpoint the protein/SAM electronic coupling site by examination of selected mutants in experiments involving variations in

alkanethiol SAM chain lengths.[8–11] As a start on work with copper proteins, we have studied four azurin mutants (W48F/Y72F/H83Q/Q107H/Y108F (all-Phe), W48F/Y72F/H83Q/Y108F/K122W/T124H, W48F/Y72F/H83Q/Q107H/Y108W and Y72F/H83Q/Q107H/Y108F), with the aim of learning about the role of Trp48 in ET to and from the copper center. Our main goal in this investigation, however, is to identify one or more strong coupling sites between the cytochrome *c* oxidase Cu$_A$ domain and various headgroups of SAMs. Subunit II (the Cu$_A$ domain) of the *ba*$_3$-type CcO from *T. thermophilus* contains a binuclear Cu$_A$ center (14.8 kDa, pI = 6.0).[23] Electrons from cyt *c*$_{552}$ pass through Cu$_A$ in subunit II to metal cofactors in subunit I of CcO, where dioxygen is reduced to water. The two copper atoms (Cu1 and Cu2) of Cu$_A$ are bridged by two cysteine thiolates (Cys149 and Cys153). In addition to two cysteine thiolates, Cu1 is coordinated by His114 and Met160 and Cu2 is coordinated by His157 and the main chain carbonyl oxygen of Gln151 (within van der Waals contact).[24,25] Iwata et al. have pointed out that His157 (His224 in subunit II of *P. denitrificans*) may be involved in ET to cyt *a* in subunit I through Arg450 (Arg473 in subunit I of *P. denitrificans*).[26]

(13) Gaigalas, A. K.; Niaura, G. *J. Colloid Interface Sci.* **1997**, *193*, 60−70.
(14) Firstrup, P.; Grubb, M.; Zhang, J.; Christensen, H. E. M.; Hansen, A. M.; Ulstrup, J. *J. Electroanal. Chem.* **2001**, *511*, 128−133.
(15) Chi, Q.; Zhang, J.; Andersen, E. T.; Ulstrup, J. *J. Phys. Chem. B* **2001**, *105*, 4669−4679.
(16) van de Kamp, M.; Floris, R.; Hali, F. C.; Canters, G. W. *J. Am. Chem. Soc.* **1990**, *112*, 907−908.
(17) Farver, O.; Blatt, Y.; Pecht, I. *Biochemistry* **1982**, *21*, 3556−3561.
(18) Groeneveld, C. M.; Canters, G. W. *J. Biol. Chem.* **1988**, *263*, 167−173.
(19) Mikkelsen, K. V.; Skov, L. K.; Nar, H.; Farver, O. *Proc. Natl. Acad. Sci. U.S.A.* **1993**, *90*, 5443−5445.

(20) Gorren, A. C. F.; den Blaauwen, T.; Canters, G. W.; Hopper, D. J.; Duine, J. A. *FEBS Lett.* **1996**, *381*, 140−142.
(21) Farver, O.; Skov, L. K.; Young, S.; Bonander, N.; Karlsson, B. G.; Vänngård, T.; Pecht, I. *J. Am. Chem. Soc.* **1997**, *119*, 5453−5454.
(22) van Pouderoyen, G.; Mazumdar, S.; Hunt, N. I.; Hill, H. A. O.; Canters, G. W. *Eur. J. Biochem.* **1994**, *222*, 583−588.
(23) Keightley, J. A.; Sanders, D.; Todaro, T. R.; Pastuszyn, A.; Fee, J. A. *J. Biol. Chem.* **1998**, *273*, 12006−12016.
(24) Williams, P. A.; Blackburn, N. J.; Sanders, D.; Bellamy, H.; Stura, E. A.; Fee, J. A.; McRee, D. E. *Nat. Struct. Biol.* **1999**, *6*, 509−516.
(25) Soulimane, T.; Buse, G.; Bourenkov, G. P.; Bartunik, H. D.; Huber, R.; Than, M. E. *EMBO J.* **2000**, *19*, 1766−1776.
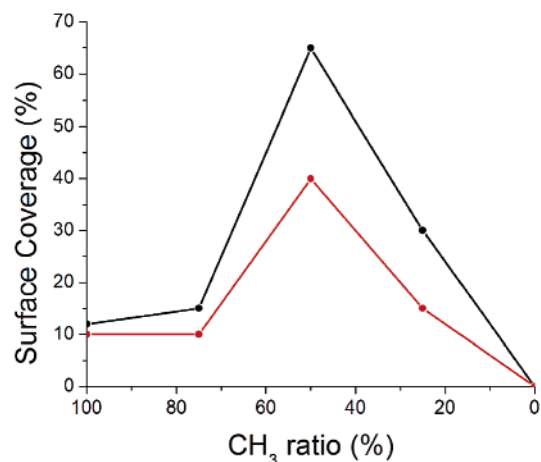
Figure 2. Variations in the amounts of immobilized azurin (black dots) and the Cu$_A$ domain of cytochrome *c* oxidase from *T. thermophilus* (red dots) on mixed [CH$_3$(CH$_2$)$_8$SH + HO(CH$_2$)$_8$SH] SAMs in 10 mM NH$_4$Ac solution at pH 4.6.

Experimental Section

Reagents: Nonanethiol, CH$_3$(CH$_2$)$_8$SH, dodecanethiol, CH$_3$(CH$_2$)$_{11}$SH, tetradecanethiol, CH$_3$(CH$_2$)$_{13}$SH, hexadecanethiol, CH$_3$(CH$_2$)$_{15}$SH, and 11-mercapto-1-undecanol, HS(CH$_2$)$_{11}$OH, were purchased from Aldrich Chemical Co. (St. Louis, MO). Tetradecanethiol, CH$_3$(CH$_2$)$_{13}$SH, was purchased from Fluka Chemie AG (Buchs, Switzerland). 8-Mercapto-1-octanethiol, HS(CH$_2$)$_8$OH, and 8-mercaptooctanoic acid, HOOC(CH$_2$)$_7$SH, were purchased from Dojindo Molecular Technology (Gaithersburg, MD). Thiols were used without further purification. Other chemicals used for preparation of buffer solutions were reagent grade.

Proteins: *P. aeruginosa* azurin was isolated and purified according to Chang et al..[27] Azurin mutants were made using Stratagene's QuikChange Multi Site-Directed Mutagenesis Kit and an inhouse azurin plasmid. Azurin mutants used were W48F/Y72F/H83Q/Q107H/Y108F (all-Phe), W48F/Y72F/H83Q/Y108F/K122W/T124H, W48F/Y72F/H83Q/Q107H/Y108W, and Y72F/H83Q/Q107H/Y108F. Water-soluble, recombinant Cu$_A$-domain of *ba$_3$*-type CcO from *T. thermophilus* was prepared according to Slutter et al..[28]

Electrodes: Gold bead electrodes were prepared by melting gold wire 99.999% from Alfa Aesar/Johnson Matthey (Ward Hill, MA) in a hydrogen flame; there were mainly two crystal surfaces, Au(111) and Au(110). The procedure for the preparation of clean gold bead electrodes has been previously reported.[29]

Mixed SAMs were prepared by immersing gold bead electrodes into mixed ethanol solutions of thiols with fixed ratios (H$_3$C−/HO−) (pure methyl, 3:1, 1:1, and 1:3 mole ratios), but SAM surface compositions were not determined. The mixed alkanethiol and ω-hydroxy alkanethiols were as follows: (i) [H$_3$C(CH$_2$)$_8$SH + HO(CH$_2$)$_8$SH], (ii) [H$_3$C(CH$_2$)$_{11}$SH + HO(CH$_2$)$_{11}$SH], (iii) [H$_3$C(CH$_2$)$_{13}$SH + HO(CH$_2$)$_{11}$SH], and (iv) [H$_3$C(CH$_2$)$_{15}$SH + HO(CH$_2$)$_{11}$SH]. Gold bead electrodes were soaked in an ethanol solution containing 200 μM ω-derivatized alkanethiols at room temperature for more than 3 h to form compact SAMs. Prior to protein immobilization the SAM-coated electrodes were activated by electrochemical treatment in 10 mM acetate buffer solution at pH 4.6.[29] Potential ranges of the oxidation−reduction cycle (ORC) are as follows: azurin and the Cu$_A$-domain of *ba$_3$* type
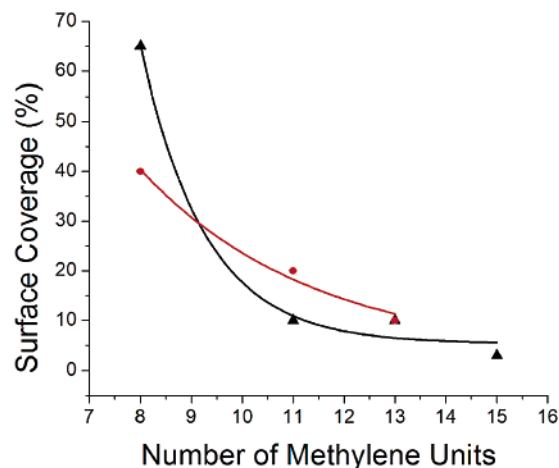

Figure 3. Amounts of immobilized azurin (black triangles) and the Cu$_A$ domain of cytochrome *c* oxidase from *T. thermophilus* (red dots) on 1:1 mixed (alkanethiol + ω-hydroxy-alkanethiol) SAMs with various chain lengths in 10 mM NH$_4$Ac solution at pH 4.6.
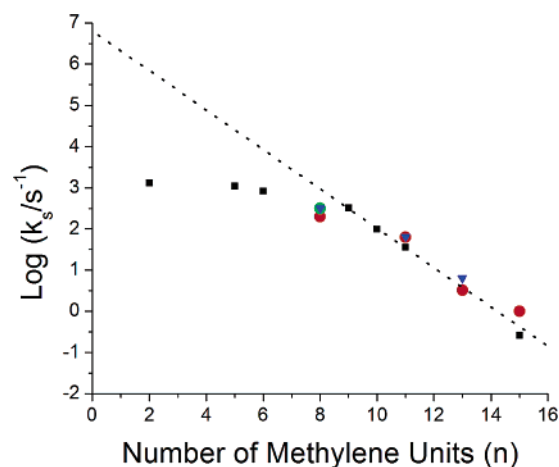

Figure 4. ET rates vs SAM chain lengths for azurin (red dots), the W48/Y72F/H83Q/Q107H/Y108F mutant (green dots), and the Cu$_A$ domain (blue downward triangles) immobilized on mixed monolayers of (alkanethiol + ω-hydroxy alkanethiol); for cyt *c* on carboxylic acid terminated alkanethiol SAM (black squares); and for the exponential decay factor β = 1.1 per CH$_2$ (••••••).[8] R^2 = 0.97 when $n \geq 9$.

CcO, 0.5 to − 0.2 V. Proteins were immobilized on the mixed SAMs by soaking the SAM-coated electrodes in about 100 μM protein solution overnight in a refrigerator. Prior to cyclic voltammetric (CV) measurements, the electrodes were thoroughly rinsed with Milli-Q water to remove excess proteins from the electrode surface.

Electrochemical Measurements: Gold bead electrode tips were immersed in electrolyte solution to minimize wire-surface effects on the measurements. Electrolyte solutions for azurin and the Cu$_A$ domain were 10 mM ammonium acetate at pH 4.6. Electrolyte solutions were deaerated with purified argon and maintained under an argon stream during the measurements. After each experiment, the SAM amount on each gold bead electrode was evaluated by cathodic stripping voltammetry in 0.5 M KOH solution in the potential range −0.5 to −1.3 V.[29,30]

ET rate constants from protein redox sites to the gold electrode through different SAMs were evaluated from CV peak separations.[31] Electrode potentials were measured against Ag/AgCl in satd. KCl (0.197

(26) Iwata S.; Ostermeler, C.; Ludwig, B.; Michel, H. *Nature* **1995**, *376*, 660−669.

(27) Chang, T. K.; Iverson, S. A.; Rodrigues, C. G.; Kiser, C. N.; Lew, A. Y. C.; Germanas, J. P.; Richards, J. H. *Proc. Natl. Acad. Sci. U.S.A.* **1991**, *88*, 1325−1329.

(28) Slutter, C. E.; Sanders, D.; Wittung, P.; Malmström, B. G.; Aasa, R.; Richards, J. H.; Gray, H. B.; Fee, J. A. *Biochemistry* **1996**, *35*, 3387−3395.

(29) Tanimura, R.; Hill, M. G.; Margoliash, E.; Niki, K.; Ohno, H.; Gray, H. B. *Electrochem. Solid-State Lett.* **2002**, *5*, E67−E70.

(30) Widrig, C. A.; Chung, C.; Porter, M. D. *J. Electroanal. Chem.* **1991**, *310*, 335−359.

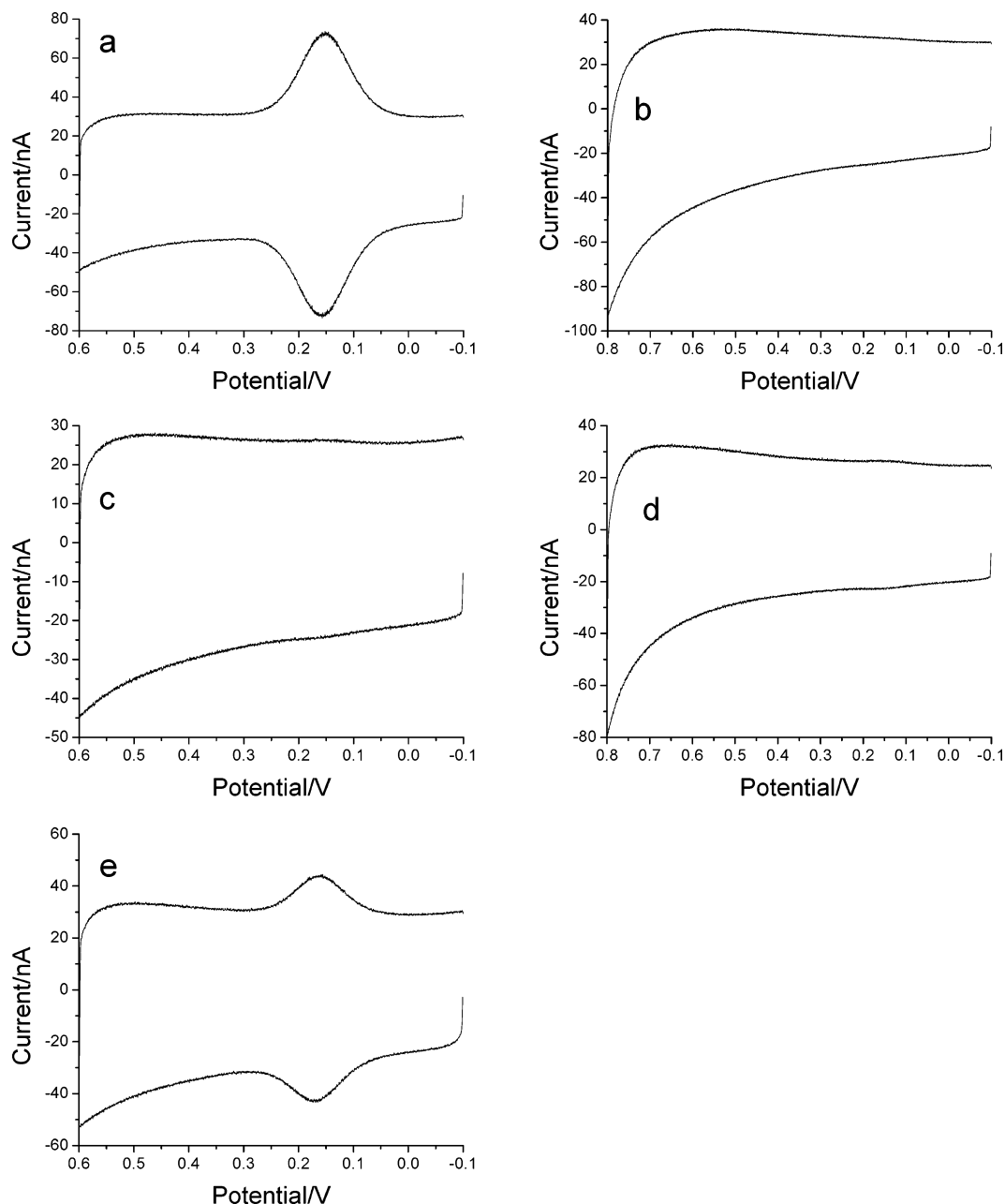(31) Laviron, E. *J. Electroanal. Chem.* **1979**, *101*, 19−28.

Figure 5. Cyclic voltammograms of azurin mutants on a 1:1 [CH$_3$(CH$_2$)$_8$SH + HO(CH$_2$)$_8$SH] SAM in 10 mM NH$_4$Ac solution at pH 4.6. Scan rate 50 mV/s; potential vs Ag/AgCl. CVs are (a) wild-type; (b) W48F/Y72F/H83Q/Q107H/Y108F mutant (All Phe); (c) W48F/Y72F/H83Q/Q107H/Y108W mutant; (d) W48F/Y72F/H83Q/Y108F/K122W/T124H mutant; (e) W48/Y72F/H83Q/Q107H/Y108F mutant (All PheW48).

V vs NHE). Cyclic voltammetry was performed using a model 660 Electrochemical Workstation (CH-Instrument, Austin, TX) at room temperature.

Results and Discussion

P. aeruginosa **Azurin.** Cyclic voltammetric measurements on *P. aeruginosa* azurin were made on pure alkanethiol SAMs and (alkanethiol + ω-hydroxy-alkanethiol) mixed SAMs in 10 mM acetate buffer solution at pH 4.6. A well-defined voltammetric response from azurin was obtained on the SAMs with different mixing ratios and chain lengths (Figure 1). The formal potential of azurin immobilized on a long chain alkanethiol SAM is about 30 mV more negative than the value reported by van de Kamp et al..[32] The amounts of immobilized azurin (Γ_{azurin}) on a mixed SAM increase proportionately with

the HO(CH$_2$)$_8$SH mole fraction, reaching an optimum on the 1:1 SAM (Figure 2); Γ_{azurin} decreases with chain length monotonically (Figure 3). Although the values of the amounts of immobilized azurin on a H$_3$C(CH$_2$)$_8$SH SAM agree reasonably well with those reported by Chi et al. on H$_3$C(CH$_2$)$_8$SH,[15] the dependence of Γ_{azurin} on chain length differs significantly. We did not find that a monotonic decrease of Γ_{azurin} with chain length accords with the solubility of alkanethiols in water (Figure 3). The difference between our results and those reported by Chi et al.[15] could be due to differences in SAM gold electrode preparations.

The formal potential estimated from the midpoint of the peak-to-peak potentials is 0.15 V vs. Ag/AgCl, which is independent of the composition of the mixed [H$_3$C(CH$_2$)$_8$SH + HO(CH$_2$)$_8$SH] monolayer, and agrees well with that obtained
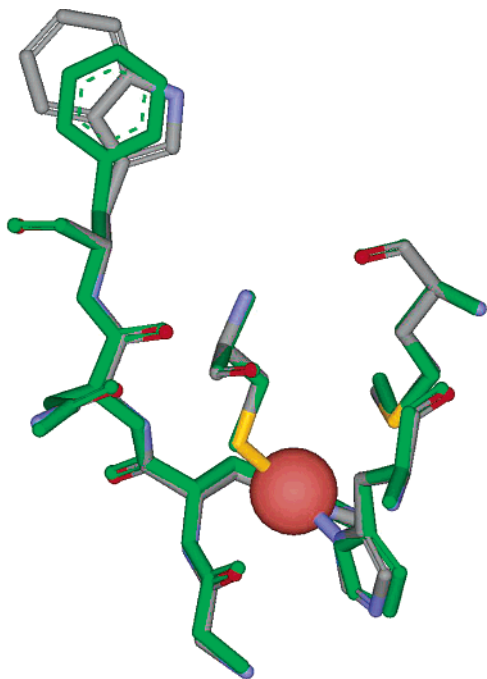
Figure 6. Overlay of the copper centers of wild-type and all Phe (in green) azurins.

by the Ulstrup group on alkanethiol SAMs[14,15] but is 40−50 mV more positive than other values.[13,32,33] The ET rate constants as a function of the number of methylene groups in the alkanethiol were evaluated using CVs.[31] A linear relationship between the logarithm of the ET rate and the chain length (for longer chains) with a slope of about $1.0/CH_2$ was obtained (Figure 4), in accordance with findings from similar work on horse heart cyt c at carboxylic acid terminated alkanethiol SAMs[9,11,34] as well as other proteins.[35,36]

A striking result is that azurin mutants become electrochemically inactive if the tryptophan at position 48 is replaced by phenylalanine (Trp48Phe). The Y72F/H83Q/Q107H/Y108F mutant showed a well-defined CV response at a formal potential of 0.16 V (Figure 5). The amount of Y72F/H83Q/Q107H/Y108F azurin immobilized on a 1:1 mixed monolayer of $[H_3C(CH_2)_8SH + HO(CH_2)_8SH]$ was about 25% of that of the wild type. Our results strongly suggest that an amino acid residue near position 48 is coupled to the methyl and hydroxy SAM headgroups. Surprisingly, hydrophobic interactions between His117 and the SAM headgroups [methyl + hydroxyl] appear not to facilitate ET to the copper center.

The structure of W48F/Y72F/Y108F/H83Q/Q107H azurin is nearly the same as that of the wild-type protein[37] (Figure 6). The very small difference in the formal potentials (<10 mV) between wild-type azurin and the mutant also suggests that the active site is minimally perturbed. A high-resolution structure of azurin in the region of the active site reveals that the coordination geometry is constrained by an extensive hydrogen bond network embedded in a cluster of hydrophobic residues.[38]

Among these residues, Asn47 and its side chain may interact with the SAM hydroxy headgroups. These interactions would facilitate ET to the copper center via the hydrogen bond between Asn47 and the sulfur atom of Cys112, forming a coupling pathway that involves only five covalent bonds (vide infra). Though causing no major structural alteration, the replacement of tryptophan by phenylalanine (W48F) may perturb the azurin structure enough such that a short SAM-to-sulfur bridge cannot be made, owing to alterations in protein dynamics that would not allow the mutant protein to maneuver into a "hot" contact position.

Azurin−SAM Electronic Coupling Site. For electron transfer between reactants in spatially fixed sites, the first-order rate constant k_{et} can be written as follows:[39]

$$k_{et} = \kappa(r)\nu_n \exp[-(\lambda + \Delta G^\circ)^2/4\lambda RT] \qquad (1)$$

where $\kappa(r)$ is the transmission coefficient when the reactants are at a distance r apart, ν_n is the nuclear frequency factor ($\nu_n = 10^{13}$ s^{-1}), λ is the reorganization energy, and ΔG° is the standard free energy of the reaction. In the nonadiabatic regime (for long-range ET processes) $\kappa(r) \ll 1$, $\kappa(r)\nu_n$ is given by ($\nu_n = 10^{13}$ s^{-1} at $r = r_0$):

$$\kappa(r)\nu_n = \nu_n \exp[-\beta (r - r_0)] \qquad (2)$$

In electrochemical measurements of ET rates at the formal potentials of the redox species, $\Delta G^\circ = 0$ and λ_{el} is one-half of that for a self-exchange reaction ($\lambda_{el} = \lambda_{11}/2$). The ET rate equation given by eq 1 becomes

$$k_{et} = \kappa(r)\nu_n \exp(-\lambda_{el}/4RT) \qquad (3)$$

The electronic coupling associated with a tunneling pathway from the redox center of the proteins through ω-derivatized alkanethiol SAMs to the electrode can be written as a product:

$$H_{AB}{}^2 \propto \kappa_{protein}\kappa_{inter}\kappa_{SAM} \qquad (4)$$

where $\kappa_{protein}$, κ_{inter}, and κ_{SAM} represent transmission coefficients, respectively, for an intramolecular ET through the protein, interface ET between the protein and the SAM headgroup, and ET through the ω-derivatized alkanethiol SAMs. Values for $\kappa_{protein}$ and κ_{SAM} have been established from many experimental investigations.[9,36,40−44]

The ET rate constants for redox proteins immobilized on SAMs are given by the following expresions:

$$k_{et} = k_o \exp[-(d_{protein}\beta_{protein} + d_{inter}\beta_{inter})] \exp[-(n + 3)\beta_{SAM}] \qquad (5)$$

$$k_o = \nu_n \exp(-\lambda_{el}/4RT) \qquad (6)$$

(32) van de Kamp, M.; Silvestrini, M. C.; Brunori, M.; Van Beeumen, J.; Hali, F. C.; Canters, G. W. *Eur. J. Biochem.* **1990**, *194*, 109−118.
(33) Battistuzzi, G.; Borsari, M.; Loschi, L.; Righi, F.; Sola, M. *J. Am. Chem. Soc.* **1999**, *121*, 501−506.
(34) Jeuken, L. J. C.; Armstrong, F. A. *J. Phys. Chem. B* **2001**, *105*, 5271−5282.
(35) Tezcan, F. A.; Crane, B. R.; Winkler, J. R.; Gray, H. B. *Proc. Natl. Acad. Sci. U.S.A.* **2001**, *98*, 5002−5006.
(36) Hsu, C.-P.; Marcus, R. A. *J. Chem. Phys.* **1997**, *106*, 584−598.

(37) Wehbi, W. A. Ph.D. Thesis, 2003, California Institute of Technology, Pasadena, CA.
(38) Crane, B. R.; Di Bilio, A. J.; Winkler, J. R.; Gray H. B. *J. Am. Chem. Soc.* **2001**, *123*, 11623−11631.
(39) Marcus, R. A.; Sutin, N. *Biochim. Biophys. Acta* **1985**, *811*, 265−322.
(40) Smalley, J. F.; Feldberg, S. W.; Chidsey, C. E. D.; Linford, M. R.; Newton, M. D.; Liu, Y.-P. *J. Phys. Chem.* **1995**, *99*, 13141−13149.
(41) Carter, M. T.; Rowe, G. K.; Richardson, J. N.; Tender, L. M.; Terrill, R. H.; Murray, R. W. *J. Am. Chem. Soc.* **1995**, *117*, 2896−2899.
(42) Wuttke, D. S.; Bjerrum, M. J.; Winkler, J. R.; Gray, H. B. *Science* **1992**, *256*, 1007−1009.
(43) Wuttke, D. S.; Bjerrum, M. J.; Chang, I. J.; Winkler, J. R.; Gray, H. B. *Biochim. Biophys. Acta* **1992**, *1101*, 168−170.
(44) Gray, H. B.; Winkler, J. R. *Annu. Rev. Biochem.* **1996**, *65*, 537−561.
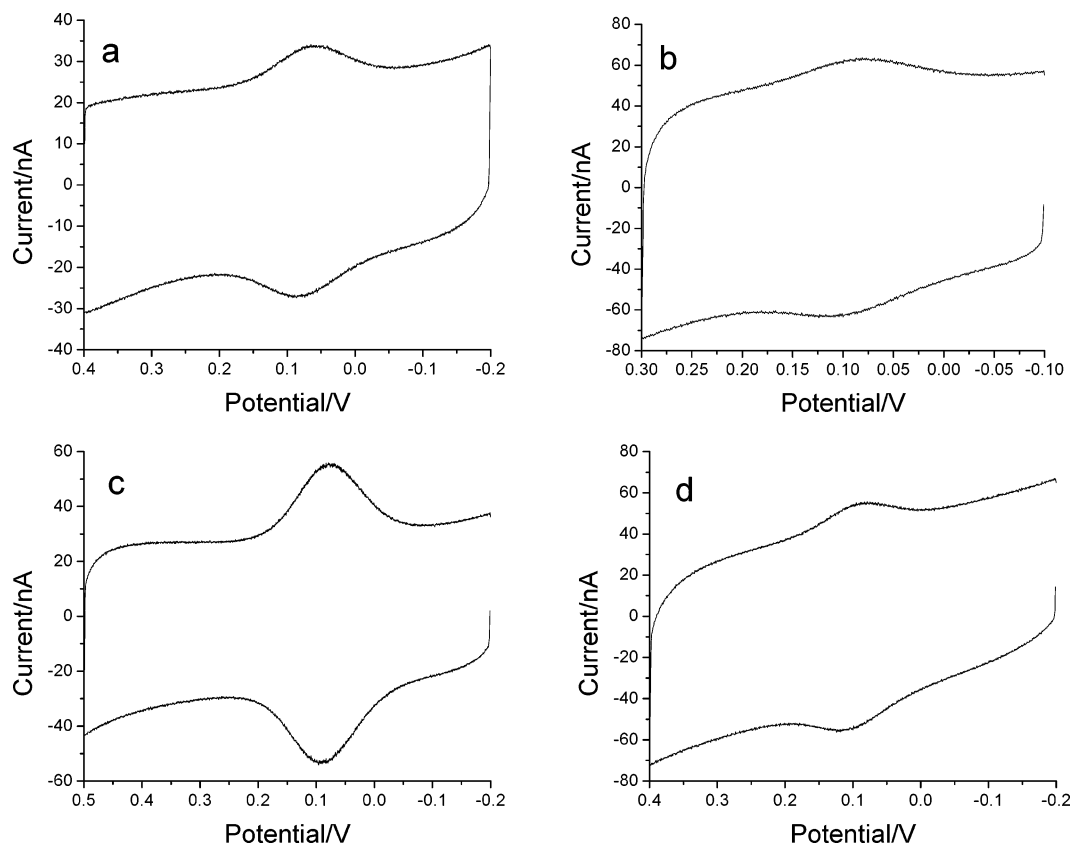
Figure 7. Cyclic voltammograms of the Cu_A domain on a [$CH_3(CH_2)_8SH$ + $HO(CH_2)_8SH$] SAM in 10 mM NH_4Ac buffer solution at pH 4.6. Scan rate 50 mV/s; potential vs Ag/AgCl. [$CH_3(CH_2)_8SH$ + $HO(CH_2)_8SH$] mixing ratio (a) 100:0; (b) 3:1; (c) 1:1; (d) 1:3.

where $d_{protein}$ represents the intramolecular ET distance from the redox center of the proteins to the electronic coupling site with the headgroup of the SAMs; d_{inter} is the intermolecular distance between the electronic coupling sites; $(n + 3)$ corresponds to the number of bonds through $HO(CH_2)_nS-$ SAM; and $\beta_{protein}$, β_{inter}, and β_{SAM} represent the exponential decay factors for intramolecular ET through the protein, for intermolecular ET through the interface, and for tunneling through the SAM, respectively.

The ET rate constant (k_{et}) through a $HO(CH_2)_{11}S-$ SAM is 63 s^{-1}; and the exponential decay factor through alkyl chains is 1.09 ± 0.02 per methylene group ($\beta_{SAM} = 0.71 \pm 0.01$ Å^{-1}), independent of the type of redox species at alkanethiol-SAMs termini for $n > 6$.[9] The maximum ET rate constant k_o ($r = r_o$) at the formal potential ($\Delta G° = 0$) is estimated from eq 6 to be 5.4×10^{11} s^{-1} at 298 K (assuming $\nu_n = 10^{13}$ s^{-1} and $\lambda_{el} = 0.3$ eV). By assuming that $\beta_{protein} \approx 1.0$/bond and ($d_{inter}\beta_{inter} \approx 3$),[42–44] we have the following:

$$63 = 5.4 \times 10^{11} \exp[-(d_{protein}\beta_{protein} + 3)] \exp(-14 \times 1.1) \quad (7)$$

$$d_{protein}\beta_{protein} = (r - r_o) = 4.5 \text{ bonds } [= 6.5 \text{ when } \lambda_{el} = 0.1 \text{ eV}] \quad (8)$$

We estimate that 4 to 5 bonds couple the protein active site to the SAM: accordingly, it appears that the electronic coupling sites of azurin and the Cu_A domain with SAM headgroups are located very near the metal centers.

Subunit II (the Cu_A Domain). Cyclic voltammetric measurements on the Cu_A domain of ba_3-type cytochrome c oxi-
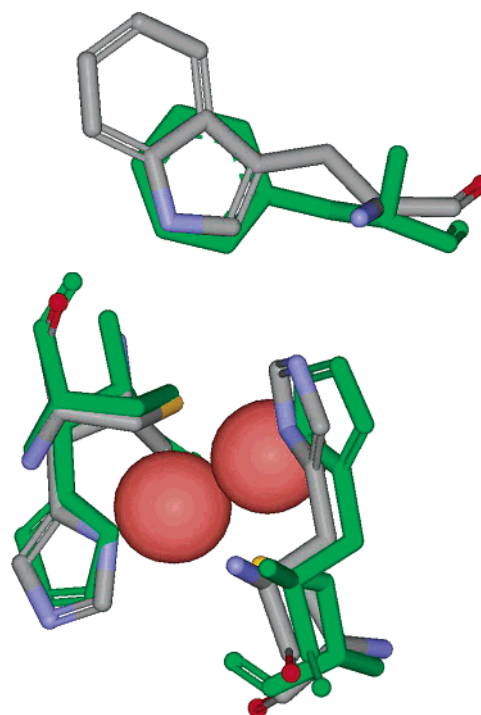

Figure 8. Cu_A domains highlighting the conformations of Trp143 (*R. sphaeroides*) and Phe88 (*T. thermophilus*) (in green).

dase from *T. thermophilus* were made on pure alkanethiol SAM and (alkanethiol + ω-hydroxy-alkanethiol) mixed SAMs with different compositions and chain lengths in 10 mM acetate buffer solution at pH 4.6. Well-defined voltammograms of the
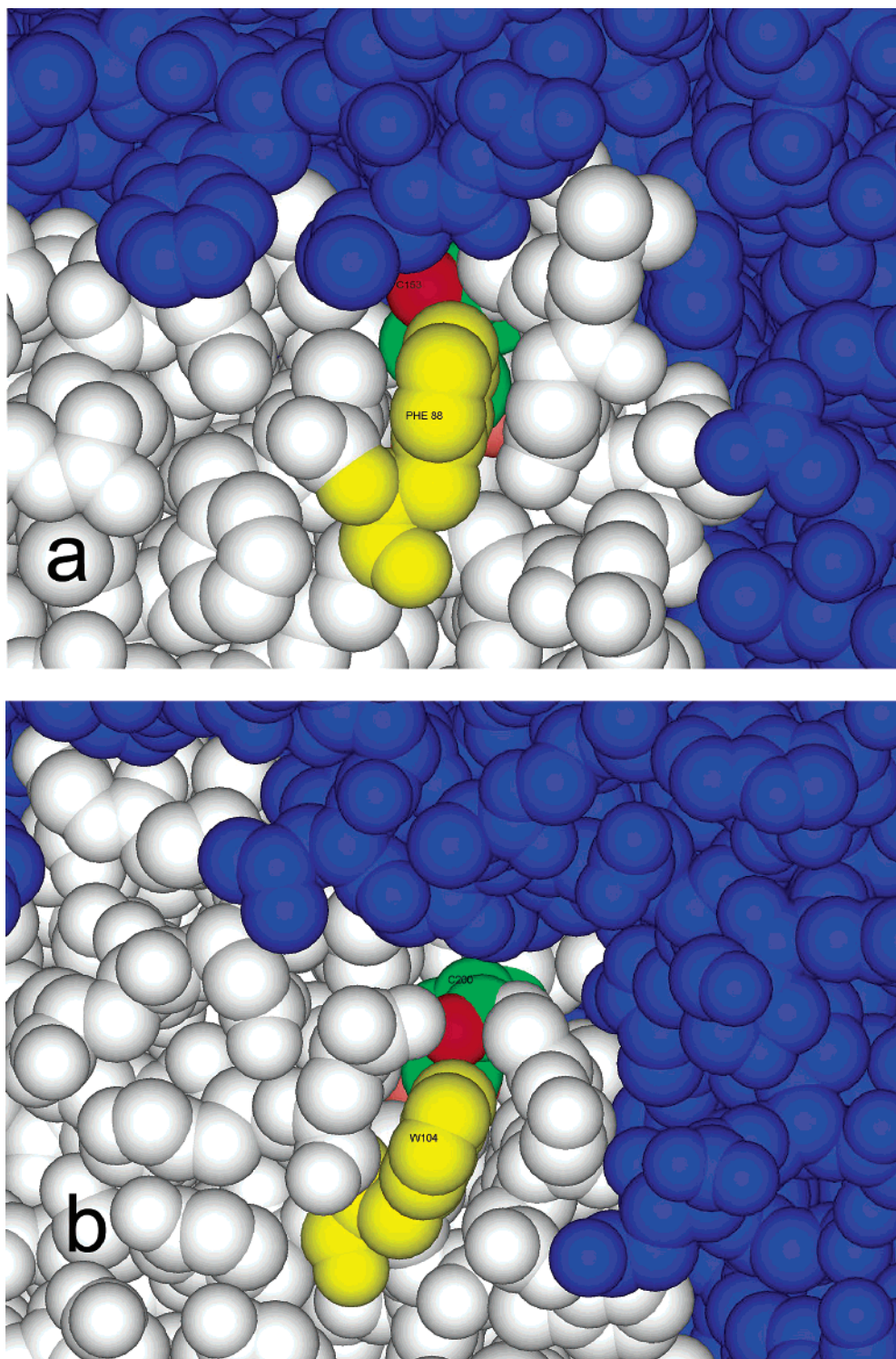
Figure 9. Structural models of the Cu$_A$ domain (white) and the CcO subunit 1 domain (blue) of (a) *T. thermophilus* (Cys153) and (b) bovine (Cys200) cytochrome *c* oxidase. W104 and F88 in yellow, C200 and C153 in green with the cysteine backbone carbonyl in red.

Cu$_A$ domain were obtained on mixed [H$_3$C(CH$_2$)$_8$SH + HO(CH$_2$)$_8$SH] (SAMs Figure 7). The amounts of immobilized Cu$_A$ (Γ_{CuA}) on a mixed SAM increase proportionately with the HO(CH$_2$)$_8$SH mole fraction, reaching an optimum on the 1:1 SAM (Figure 2); Γ_{CuA} decreases with chain length monotonically (Figure 3) as in the case of azurin. The adsorption behavior of the Cu$_A$ domain on the SAMs suggests that the interaction between the headgroups of the SAMs and the Cu$_A$ domain is similar to that with azurin (Figures 2 and 3). The formal potential

estimated from the midpoint of the peak-to-peak potentials is 0.10 V vs Ag/AgCl, which is about 0.06 V more negative than the value determined in solution at pH 8.[45] The ET rate constants with respect to the number of methylene groups in the alkanethiol were evaluated using CVs,[31] and a linear relationship was found between the logarithm of the ET rate vs chain length (for longer chains), with a slope of about 1.0/CH$_2$ (Figure 4).

(45) Immose, C.; Hill, M. G.; Sanders, D.; Fee, J. A.; Slutter, C. E.; Richards, J. H.; Gray, H. B. *JBIC* **1996**, *1*, 529−531.

These values agree well with previous studies on cyt *c* (and its mutants) on carboxylic acid terminated alkanethiol SAMs.[9−11] The Cu$_A$ domain did not show visible voltammetric responses on the pure ω-hydroxy-alkanethiol SAM.

Electron-transfer reactions in cytochrome *c* oxidase are facilitated by low reorganization energies.[46−48] The reorganization energy and the ET path distance from the headgroup of the SAM to the Cu$_A$ domain are similar to those of azurin (ET kinetics profiles of these proteins are nearly the same, Figure 4). The upper limit for the reorganization energy of the Cu$_A$ domain on the SAM [$\sim$0.3 eV $(= \lambda_{11}/2)$] is just above the value of 0.4 eV for purple azurin estimated from pulse radiolysis kinetics experiments.[49] This relatively low reorganization energy, which likely is due hydrophobic coupling of the Cu$_A$ domain to the SAM, mimics the biological situation in which the barrier to ET between two proteins (cyt c_{552} and the Cu$_A$ domain of *T. thermophilus* CcO) is greatly lowered upon complex formation.

Three segments in the amino acid sequences in subunit II (the Cu$_A$ domain) of *T. thermophilus* CcO are involved in complex formation with cyt c_{552}.[24,25] The segment I sequence (Ala87, Phe88, Gly89, and Tyr90 of *T. thermophilus*) is strictly conserved among bovine, *R. sphaeroides*, and *P. denitrificans* CcOs). Conserved sequences in segment II (Asp111, Val112, Ile113, and His114) also are important in the cytochrome *c* oxidase molecule (the subunit I/subunit II complex). In the subunit I/subunit II complex, Asp111, Val112, Pro129, and Gly130 in subunit II (the Cu$_A$ domain) interact with four strictly conserved residues (Tyr136, Pro137, Pro138, Leu139) in subunit I.[24] Segment III in the Cu$_A$ domain consists of amino acids with uncharged groups (the loop from Gly154 to Met160) and is accessible to solvent in the cytochrome *c* oxidase molecule. His157, which is located next to segment III, could be an electronic coupling site with subunit I.[26,46,47]

For CcOs from bovine, *R. sphaeroides*, and *P. denitrificans*, a conserved tryptophan residue (Trp104 in bovine, Trp143 in *R. sphaeroides*, and Trp121 in *P. denitrificans*) in segment I plays an important role in facilitating intermolecular ET.[50−57] The replacement of tryptophan by phenylalanine, Trp143Phe, in subunit II of *R. sphaeroides* markedly decreases the intermolecular ET rate with horse heart cyt *c* (8.4×10^{-4} slower with Trp143Ala and 2.2×10^{-3} slower with Trp143Phe[50,51,55]). The Cu$_A$ ligands of both *T. thermophilus* and *R. sphaeroides*

are shown in Figure 8 together with Phe88 of *T. thermophilus* and Trp143 of *R. sphaeroides*. Both Phe88 and Trp143 have parallel and nearly superimposable orientations. It is reasonable to assume that the environment of the Trp143Phe *R. sphaeroides* Cu$_A$ center and the ET pathway from cyt *c* (or other physiological redox partner) are the same as those of the native protein. That is, the through space ET distances in the native protein and the Trp143Phe mutant should be virtually the same. Solomon and co-workers modified the ET pathway proposed by Wang et al.[51] and Roberts and Pique[52] by taking into account the docking structure between cyt *c* and CcO and the covalency of the Cu−S(Cys) bond to rationalize the experimental data.[58,59] This modified ET pathway involves a van der Waals contact between the heme methyl group (CBC) of cyt *c* and the indole ring (CZ3) of Trp104 of bovine CcO (Trp143 of *R. sphaeroides* CcO) and a hydrogen bond between NE1 of Trp104 and the main chain carbonyl oxygen of Cys200 (Cys256 of of *R. sphaeroides* CcO).[58,59]

One question remains: how could ET in *T. thermophilus* CcO be efficiently mediated by Phe88 instead of the tryptophan residue found in other CcOs. Note that the structures of the Cu$_A$ domain of CcOs from both *T. thermophilus* and *R. sphaeroides* in the vicinity of Phe88 (Trp143) and Cys153 (Cys256) are similar. Could, for example, a small perturbation of the environment in the vicinity of Cys256 by the mutation of Trp143 in the Cu$_A$ domain of *R. sphaeroides* CcO give rise to a significant decrease in the ET rates from cyt *c* to CcO by causing a structurally small perturbation of the environment in the vicinity of Cys256 even though the ET pathway does not directly involve Trp143 (or Phe88)? We think so: segment III, which, in intact CcO (subunit I/subunit II complex), is accessible to solvent, is effectively buried at the interface of the cyt c_{552}/CcO complex. The interaction domains form a pocket between the loops from Ala87 to Tyr90 (segment I) and from Cys153 to Leu155, and in this region the main chain carbonyl oxygen of Cys153, which is strictly conserved, is accessible and could form a hydrogen bond with the SAM ω-hydroxy group (Figure 9), producing a four-bond electronic coupling pathway from the carbonyl oxygen to the Cys153 sulfur atom that would lead to rapid intermolecular ET. Accordingly even small structural perturbations in the region of the Cys153 carbonyl oxygen could dramatically affect the coupling to the Cu$_A$ active site.

(46) Ramirez, B. E.; Malmström, B. G.; Winkler, J. R.; Gray, H. B. *Proc. Natl. Acad. Sci. U.S.A.* **1995**, *92*, 11949−11951.
(47) Regan, J. J.; Ramirez, B. E.; Winkler, J. R.; Gray, H. B.; Malmström, B. G. *J. Bioenerg. Biomembr.* **1998**, *30*, 35−39.
(48) Hoke, K. R. Ph.D. Thesis, 2002, California Institute of Technology, Pasadena, CA.
(49) Farver, O.; Lu, Y.; Ang, M. C.; Pecht, I. *Proc. Natl. Acad. Sci. U.S.A.* **1999**, *96*, 899−902.
(50) Zhen, Y.; Hoganson, C. W.; Babcock, G. T.; Ferguson-Miller, S. *J. Biol. Chem.* **1999**, *274*, 38032−38041.
(51) Wang, K.; Zhen, Y.; Sadoski, R.; Grinnell, S.; Geren, L.; Ferguson-Miller, S.; Durham, B.; Millett, F. *J. Biol. Chem.* **1999**, *274*, 38042−38050.
(52) Roberts, V. A.; Pique, M. E. *J. Biol. Chem.* **1999**, *274*, 38051−38060.
(53) Witt, H.; Malatesta, F.; Nicoletti, F.; Brunori, M.; Ludwig, B. *Eur. J. Biochem.* **1998**, *251*, 367−373.
(54) Witt, H.; Malatesta, F.; Nicoletti, F.; Brunori, M.; Ludwig, B. *J. Biol. Chem.* **1998**, *273*, 5132−5136.
(55) Millett, F.; Durham, B. *Biochemistry* **2002**, *41*, 11315−11324.
(56) Drosou, V.; Malatesta, F.; Ludwig, B. *Eur. J. Biochem.* **2002**, *269*, 2980−2988.
(57) Flöck, D.; Helms, V. *Proteins* **2002**, *47*, 75−85.
(58) Gamelin, D. R.; Randall, D. W.; Hay, M. T.; Houser, R. P.; Mulder, T. C.; Canters, G. W.; de Vries, S.; Tolman, W. B.; Lu, Y.; Solomon, E. I. *J. Am. Chem. Soc.* **1998**, *120*, 5246−5263.
(59) George, S. D.; Metz, M.; Szilagyi, R. K.; Wang, H.; Cramer, S. P.; Lu, Y.; Tolman, W. B.; Hedman, B.; Hodgson, K. O.; Solomon, E. I. *J. Am. Chem. Soc.* **2001**, *123*, 5757−567.